Stark-broadening measurements of $3d \rightarrow nf$ transitions in lithiumlike and heliumlike ions

J. C. Moreno and H. R. Griem
Laboratory for Plasma Research, University of Maryland, College Park, Maryland 20742

R. W. Lee
Lawrence Livermore National Laboratory, Livermore, California 94550

J. F. Seely
Naval Research Laboratory, Washington, D.C. 20375
(Received 1 July 1992)

We report here on high-resolution spectral measurements of Stark-broadened $3d$-$5f$ lines from lithiumlike ions and $3d$-$4f$ lines from heliumlike ions. The spectra were emitted from high-density laser-produced plasmas. Plasmas were produced by irradiating thin- and thick-foil targets made of magnesium, aluminum, phosphorus, and chlorine with the OMEGA laser in a line-focus geometry. Line profiles were compared to a Stark-broadening calculation that uses the static-ion approximation and an impact approximation for the electrons. The dependence of Stark broadening on atomic number is discussed. For the aluminum plasmas $\sim 10\%$ narrowing was observed in the width of the $3d$-$5f$ line as the length of the plasma was increased from 3 to 6 mm.

PACS number(s): 32.70.Jz, 52.25.Nr, 52.70.La

I. INTRODUCTION

Spectroscopic measurements of plasmas have proven to be an important method of diagnosing plasma parameters. Line-profile measurements are particularly relevant to understanding the properties of laser-produced plasmas, such as occur in inertial confinement fusion and x-ray-laser research. The principal mechanisms that influence the line shape for these high-density plasmas are Doppler broadening (both thermal and motional), Stark broadening due to microfields in the plasma, and opacity broadening due to absorption of the emission as it traverses the plasma. In this paper we will discuss profile measurements of $3d$-$5f$ lines of lithiumlike magnesium, aluminum, phosphorus, and chlorine from laser-produced plasmas, as well as $3d$-$4f$ lines of heliumlike magnesium and aluminum from the same plasmas. These lines are strongly influenced by Stark broadening for $N_e \gtrsim 10^{19}$ cm^{-3}.

The $3d$-$5f$ and $3d$-$4f$ lines of lithiumlike ions have been studied extensively as soft-x-ray-lasing transitions and gain has been observed in several experiments using line-focused laser-produced plasmas [1–4]. Population inversion is produced in this case as the plasma cools through three-body recombination, which preferentially populates the high-n quantum number levels. Line broadening of these transitions can seriously affect the achievable gain, and therefore measurements of line profiles are an important part of x-ray-laser research. Indeed, the importance of x-ray-laser linewidths has resulted in renewed interest in high-resolution spectral measurements of lasing lines [4–6]. As these x-ray lasers approach saturation, it is predicted that additional broadening may occur due to the interaction between ions and the laser field (power broadening) [7].

There have been several recent experiments that included Stark-broadening measurements of highly charged ions in high-density plasmas. The line profiles of Balmer alpha (H_α) lines, which are also of interest for x-ray lasers, have been measured for B V and C VI, and a Stark-width scaling with electron density and atomic number has been proposed [8, 9]. A gas-liner pinch was used to measure $3s$-$3p$ line profiles of C IV, N V, and O VI showing a Z_i^{-1} dependence of the Stark width on ionization stage Z_i in disagreement with Stark-broadening calculations using the electron-impact approximation [10]. This experiment has been extended recently to Ne VIII [11]. The same gas-liner pinch was used to measure spectral line shapes of $3p$-$4d$, $3d$-$4f$, $4d$-$5f$, and $4f$-$5g$ transitions in Li-like C IV and N V [12]. Asymmetric Stark profiles of Li-like ions were observed from plasmas created by a picosecond KrF laser [13]. In a related laser-produced plasma experiment, electron densities inferred from Stark broadening of Li-like transitions were found to be inversely proportional to the lifetimes of the upper levels of the transitions [14]. Li-like and Be-like krypton spectra were obtained from implosion experiments using gas-filled microballoons as targets [15]. Good agreement was observed between measured spectral lines and the Stark-broadening model of Woltz and Hooper.

In this paper we discuss high-resolution measurements of Stark-broadened Li-like $3d$-$5f$ and He-like $3d$-$4f$ line profiles. Section II describes the experimental setup, including the laser system and the spectrograph. Section

III contains comparisons of experimental line profiles and simulated line profiles using a detailed numerical model for Stark broadening. Scaling of the linewidths with atomic number is also discussed.

II. EXPERIMENT

Cylindrical plasmas were produced for these measurements by using up to eight line-focused beams from the OMEGA Nd:glass laser system at a wavelength of 351 nm. A schematic of the experimental setup is shown in Fig. 1. Typical pulse lengths were 650 ps, while the laser irradiance was 8×10^{13} W/cm^2. Each beam was focused to a spot approximately 1.5 mm long and 100 μm wide, using an $f/3.7$ fused-silica lens combination consisting of a high-power aspheric singlet lens and a closely coupled cylindrical corrector plate. Flat targets, employed for the magnesium and aluminum measurements, consisted of a 0.5-μm layer of Mg or Al and a 0.01-μm layer of gold coated on a 10-μm-thick Mylar backing. For phosphorus and chlorine measurements we used thin targets with a total thickness of $\sim$0.25 μm. The phosphorus emission came from a target consisting of a Formvar foil coated with a thin film of KH_2PO_4, while the chlorine emission was from Saran ($C_2H_2Cl_2$). In this laser setup both sides of the target were illuminated by equal symmetric beams.

A 3-m grazing-incidence spectrograph was used to record spectra on Kodak 101-05 photographic plates in the range 30–300 Å [16, 17]. For these measurements a 1200-grooves/mm grating with a blaze wavelength of 120 Å was used. The entrance slit had a width of 10 μm, which gives an instrumental linewidth of 0.02 Å at a wavelength of 100 Å, i.e., a resolution of $\lambda/\Delta\lambda = 5000$. Targets were precisely positioned relative to the spectrograph so that the spectrograph view was along the axis of the cylindrical plasma. Plasma xuv emission was focused onto the entrance slit of the spectrograph by a grazing-incidence mirror. The entrance slit and the surface of the focusing mirror were rotated approximately 1° with respect to each other (around the cylindrical axis), allowing spatial resolution of the spectral emission in the direction perpendicular to the planar targets. Spectra from these experiments have already been used to measure accurate wavelengths for xuv transitions of Li-like lines of P, S, Cl, and K [18] and H-like and He-like lines of Mg and Al [19, 20].

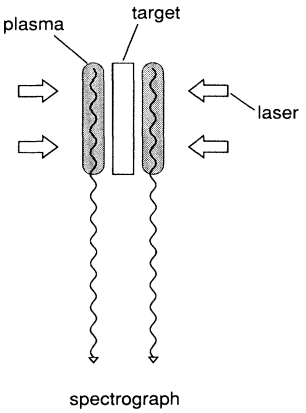

FIG. 1. Experimental setup showing line-focus irradiation of both sides of the target. The spectrograph "views" emission along the line focus.

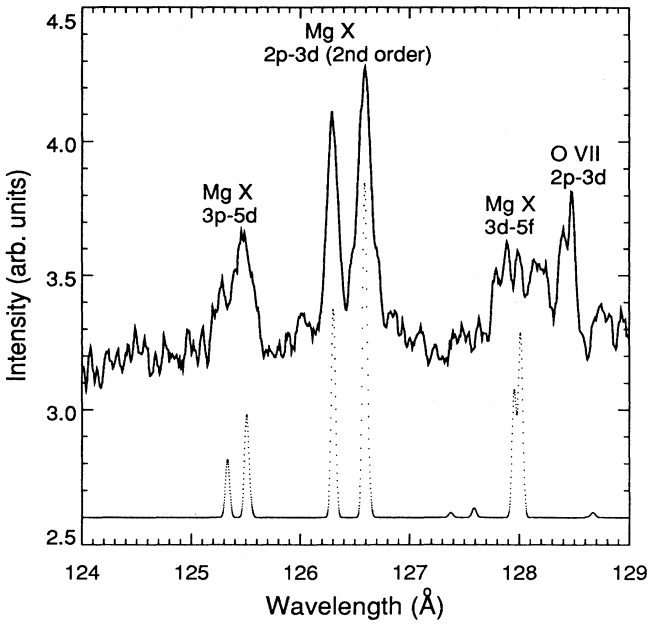

FIG. 2. Mg X spectrum showing $3p$-$5d$, $2p$-$3p$, and $3d$-$5f$ lines. The solid curve is experimental data, while the dotted curve is a simulated spectrum including only instrumental and Doppler broadening (assuming $T_i = 200$ eV).

In Fig. 2 we show an example of a measured Mg spectrum containing Li-like $3p$-$5d$, $2p$-$3d$ (second order), and $3d$-$5f$ lines compared to a simulated spectrum assuming only thermal Doppler broadening and instrumental broadening. Opacity effects and motional Doppler broadening can explain the slight broadening of the $2p$-$3d$ line; however, we attribute the substantial additional broadening of the $3p$-$5d$ and $3d$-$5f$ lines to Stark broadening. It should be noted that the $3d$-$5f$ line actually consists of three allowed transitions between the $3d$ and $5f$ levels. The other unmarked lines in this spectrum are from Be-like and B-like ions of magnesium. Intensity calibration was assumed to be linear with film density since all lines measured here had a film density <0.5 [21]. Higher-order diffraction effects from the grating increase the background level somewhat, but do not affect the line-profile measurements since there is no overlap with higher-order lines. Photographic plates were used here and therefore these measured spectra are all time integrated.

III. DISCUSSION

Analysis of line profiles from high-density plasmas must include consideration of several line-broadening mechanisms [22]. Thermal Doppler broadening for the

plasmas observed here produces a Gaussian profile with a linewidth at $\lambda = 100$ Å of 0.02 Å assuming a nuclear charge of $Z = 13$ and an ion temperature of $T_i = 200$ eV. This is an order of magnitude less than Stark broadening for these plasma conditions. Large plasma flows can produce motional Doppler broadening from Doppler shifts in several directions. In this case the spectrograph is viewing the plasma at right angles to the mostly radial plasma expansion, and therefore motional Doppler effects are minimized. However, end effects from the line focus may still contribute some broadening from Doppler shifts. Broadening due to opacity of the plasma is expected to be negligible for the $3d$-$5f$ lines.

In laser-produced plasmas, the densities are high enough that microfields in the plasma can broaden lines through the Stark effect [23]. The Stark-broadening model employed here uses the static-ion approximation and an impact approximation for the electrons [24]. An average is performed over the static-ion microfield distribution using the adjustable-parameter exponential approximation (APEX) [25]. This method allows for rapid numerical calculations of the line profile.

In Fig. 3(a) we show a comparison between a measured profile of Al XI $3d$-$5f$ and a simulation using our numerical model for Stark broadening and Doppler broadening. Good agreement is obtained between experiment and model for $N_e = 10^{20}$ cm^{-3} and $T_i = 200$ eV. The plasma was produced by using a line-focus (100 μm wide by 3 mm long) irradiation of a foil target. The same numerical calculation of the $3d$-$5f$ line profile is now compared to a spectrum from a longer-line-focus plasma (100 μm wide by 6 mm long) in Fig. 3(b). Gain was observed [1] in this measurement of the $3d$-$5f$ line intensity, which, in turn, should produce gain narrowing of the line profile. The $3d$-$5f$ line width is indeed narrower by ~10% from the case with a shorter line focus. Some narrowing may also occur if motional Doppler broadening is less in longer-line-focus experiments due to smaller end effects. A measurement of a higher-Z ion, in this case Cl XV $3d$-$5f$, is shown in Fig. 4 along with a comparison to our numerical model. A somewhat larger density, $N_e = 3 \times 10^{20}$ cm^{-3}, was required in the calculation to get good agreement with the observed profile of Cl XV. In all cases the general structure of the calculated profiles

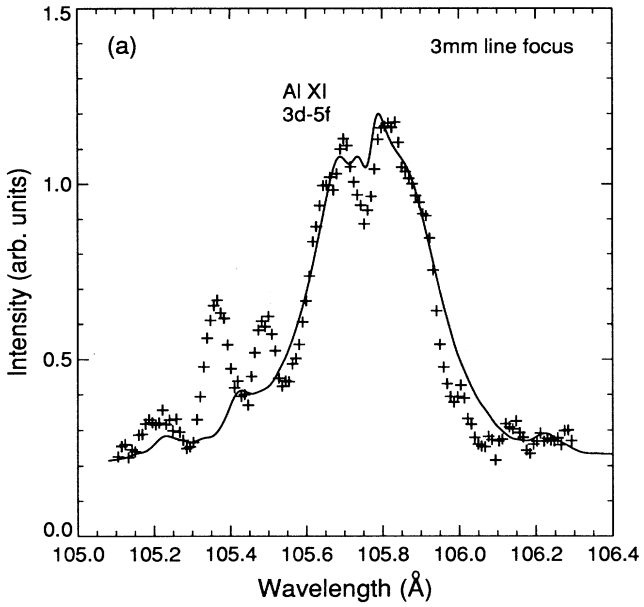

FIG. 3. Al XI $3d$-$5f$ line profile for two line-focus lengths, (a) 3 mm and (b) 6 mm. The pulses are the experimental points and the solid line is the numerical calculation for $T_i = 200$ eV and $N_e = 10^{20}$ cm^{-3}.

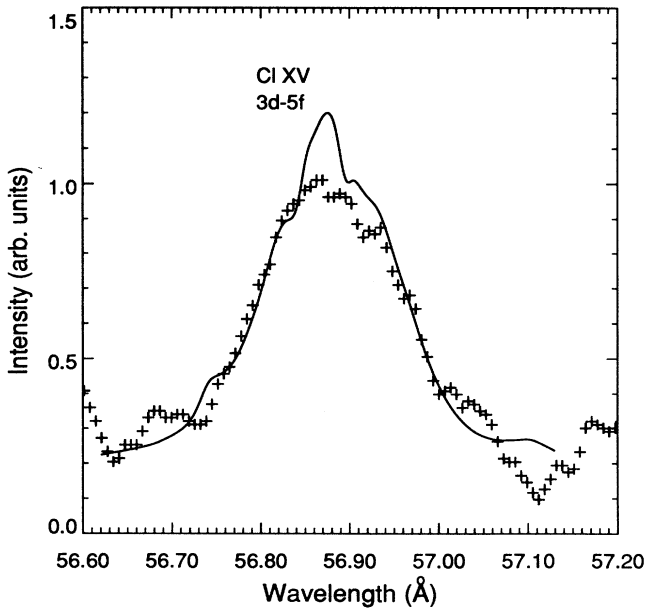

FIG. 4. Cl XV $3d$-$5f$ line profile. The pluses are the experimental points and the solid line is the numerical calculation for $T_i = 200$ eV and $N_e = 3 \times 10^{20}$ cm^{-3}.

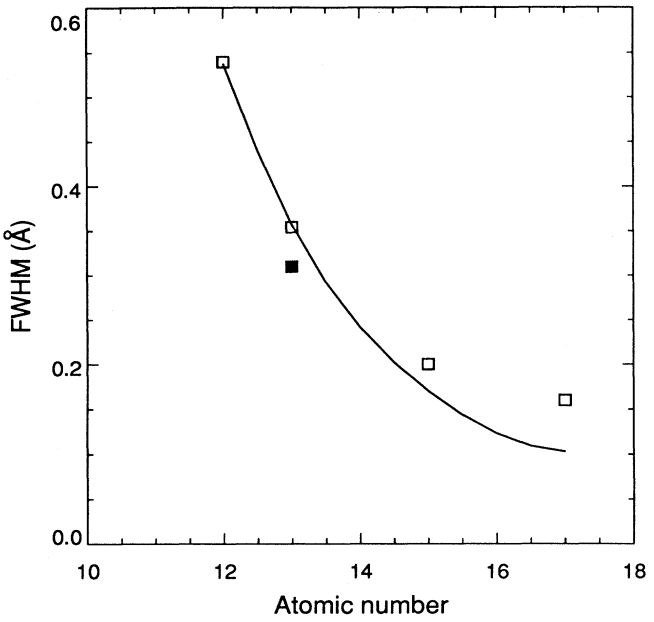

FIG. 5. Full width at half maximum of $3d$-$5f$ lines as a function of atomic number. The squares are experimental points and the solid curve is from the numerical model assuming $T_i = 200$ eV and $N_e = 10^{20}$ cm^{-3}. For aluminum ($Z = 13$), the open square is for a plasma length of 3 mm and the solid square is for a plasma length of 6 mm.

agreed well with observations. Densities inferred from these Stark-broadening calculations are about a factor of 2 larger than densities calculated previously by scaling in Z from He II [1]. However, this is not unexpected since the He II 3-5 line was calculated assuming a linear Stark effect, which is generally not valid for the electric microfields in Li-like Mg to Cl $3d$-$5f$ lines. Inclusion of ion dynamics has only a marginal effect on the width for these lines [26].

Figure 5 shows a plot of the measured full width at half maximum (FWHM) of $3d$-$5f$ line profiles of four lithium-like ions as a function of the atomic number. These are from profiles measured at a distance of $\sim$200 μm from the target surface and averaged over a $\sim$200-μm radial extent. For comparison, the solid curve in Fig. 5 is the numerical calculation assuming the same density $N_e = 10^{20}$

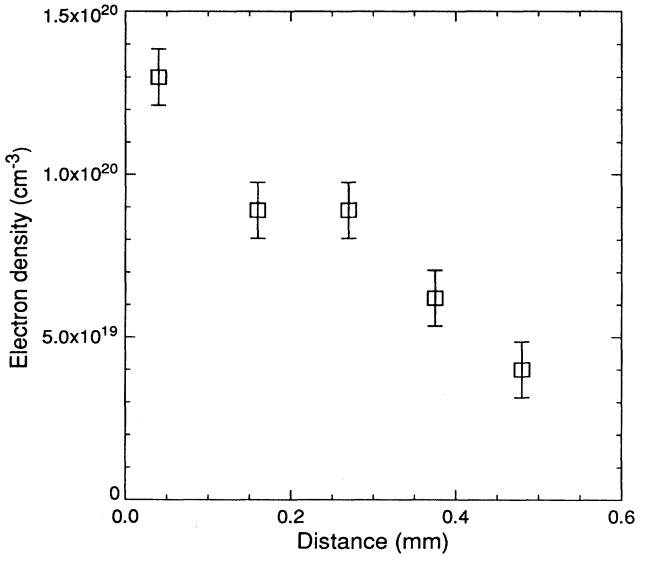

FIG. 6. Time-integrated electron density as a function of distance from the target surface. The density was inferred from the width of the Al XI $3d$-$5f$ line.

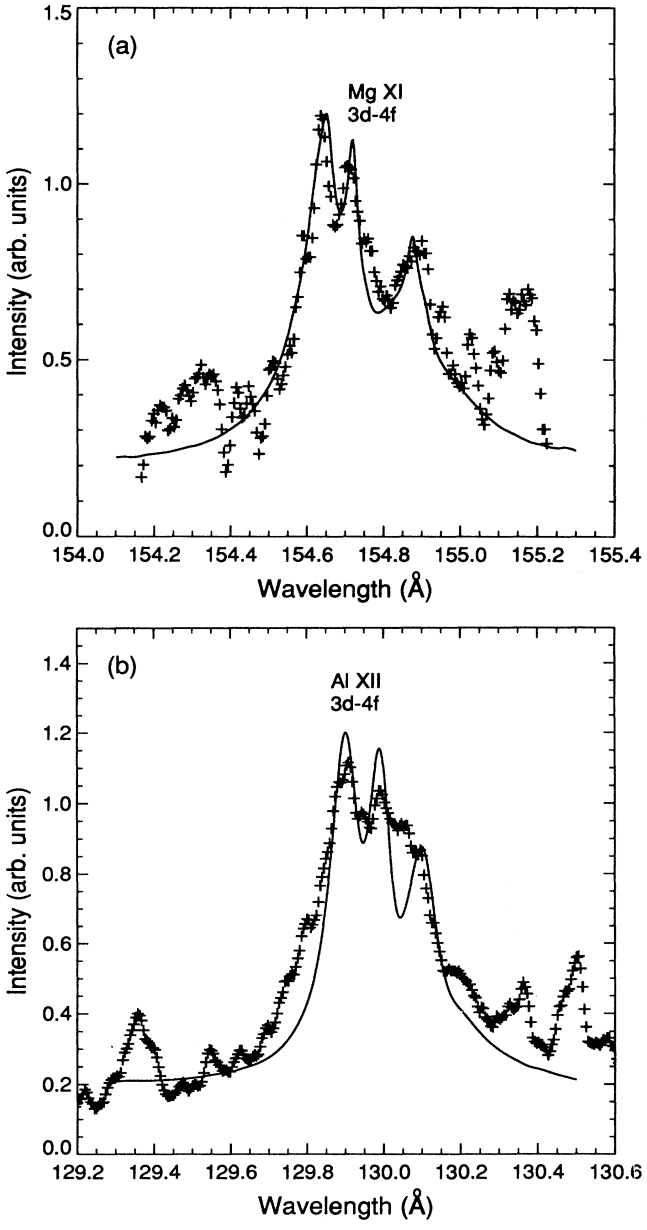

FIG. 7. Heliumlike $3d$-$4f$ line profiles for two ions (a) Mg XI and (b) Al XII. The pulses are the experimental points and the solid line is the numerical calculation for $T_i = 400$ eV and $N_e = 10^{20}$ cm^{-3}.

cm^{-3} and temperature $T_i = 200$ eV for all cases. The solid square is for the case where gain was observed, and the observed linewidth was reduced. Note that for this temperature and density the agreement with the numerical model is good for Mg and Al, but for the two higher-Z elements (P and Cl), a higher density is required in the numerical model.

Several factors may be contributing to the density variation in Fig. 5. First, P and Cl plasmas were produced using very thin foil targets irradiated from both sides. These thin foil targets resulted in higher-density plasmas with smaller density gradients than the thick foil targets of Mg and Al. By measuring the linewidth at different vertical positions along the line, we obtained spatially resolved linewidths with $\sim$100 μm spatial resolution. An indication of the density gradient can be seen in Fig. 6, which has a plot of the time-integrated electron density, using the width of the Al XI $3d$-$5f$ line, as a function of distance from the target. For P XIII and Cl XV there was little variation in the linewidth over the observable range, indicating a smaller variation in plasma density.

Another important point is that for the $3d$-$5f$ line the Stark width should scale with atomic number as Z^{-5}. The actual curve in Fig. 5 does not fit this scaling, mainly because Doppler broadening is also included. Since the ionization energies increase with Z, presumably the emission from P XIII and Cl XV should come from a higher-temperature plasma region than Mg X and Al XI. Taking into account the increased Doppler broadening would give better agreement between the model and experiment. Calculated Stark broadening alone depends only very weakly on temperature.

Heliumlike $3d$-$4f$ lines from these same plasmas also exhibit broadening due to the Stark effect. In Fig. 7 we show measured profiles of Mg XI and Al XII compared to the numerical model for Stark broadening. The structure of these lines is more complicated since there are both singlet and triplet levels, but again we see good agreement with the model using the same electron density (10^{20} cm^{-3}) as for the Li-like ions. A higher temperature (400 eV) was used for the He-like ions because of their much higher ionization potentials. He-like lines were only evident in the magnesium and aluminum plasmas. Plasma temperatures were most likely not high enough to create significant densities of He-like phosphorus and chlorine.

IV. CONCLUSION

Line profiles of Li-like $3d$-$5f$ lines were measured for a sequence of ions. These measured profiles show generally good agreement with a numerical model for Stark broadening with appropriate choice of electron density. The density variation as a function of Z can be explained by differences in the target and plasma conditions. Profile measurements of Stark-broadened He-like $3d$-$4f$ lines were consistent with assumed electron densities for Li-like ions. In general, measured line profiles of transitions in highly charged ions, which are dominated by Stark broadening, can be adopted as a diagnostic for measuring electron densities. These linewidth measurements are also valuable for understanding the gain characteristics of x-ray lasers. The narrowing of the Al XI line with an increase in plasma length could be due to gain narrowing [5] and a reduction in end effects due to motional Doppler broadening.

ACKNOWLEDGMENTS

We thank the University of Rochester laser operations staff and experimental diagnostics staff for their excellent support. We would also especially like to thank A. Calisti, B. Talin, and R. Stamm of the Université de Provence in Marseille for carrying out Stark-broadening calculations. The research and materials incorporated in this work were partially developed at the National Laser Users Facility at the University of Rochester's Laboratory for Laser Energetics, with financial support from the U.S. Department of Energy through Contract No. DEAS08-86DP-10554.

[1] J. C. Moreno, H. R. Griem, S. Goldsmith, and J. Knauer, Phys. Rev. A **39**, 6033 (1989).
[2] P. Jaegle, G. Jamelot, A. Carillon, A. Klisnick, A. Sureau, and H. Guennou, J. Opt. Soc. Am. B **4**, 563 (1987).
[3] D. Kim, C. H. Skinner, A. Wouters, E. Valeo, D. Voorhees, and S. Suckewer, J. Opt. Soc. Am. B **6**, 115 (1989).
[4] P. X. Lu, Z. Q. Zhang, Z. Z. Xu, P. Z. Fan, S. S. Chen, and B. F. Shen, Appl. Phys. Lett. **60**, 1649 (1992).
[5] J. Koch, B. J. MacGowan, L. B. DaSilva, D. L. Mathews, J. H. Underwood, P. J. Batson, and S. Mrowka, Phys. Rev. Lett. **68**, 3291 (1992).
[6] Y. Kato *et al.*, Proc. SPIE **1551**, 56 (1992).
[7] H. R. Griem and J. C. Moreno, Phys. Rev. A **44**, 4564 (1991).
[8] J. S. Wang, H. R. Griem, Y. W. Huang, and F. Böttcher, Phys. Rev. A **45**, 4010 (1991).
[9] E. J. Iglesias and H. R. Griem, Phys. Rev. A **38**, 308 (1988).
[10] F. Böttcher, P. Breger, J. D. Hey, and H.-J. Kunze, Phys. Rev. A **38**, 2690 (1988).
[11] S. Glenzer, N. I. Uzelac, and H.-J. Kunze, Phys. Rev. A **45**, 8795 (1992).
[12] F. Böttcher, J. Musielok, and H.-J. Kunze, Phys. Rev. A **36**, 2265 (1987).
[13] C. H. Nam, W. Tighe, S. Suckewer, J. F. Seely, U. Feldman, and L. A. Woltz, Phys. Rev. Lett. **59**, 2427 (1987).
[14] J. F. Seely, U. Feldman, C. H. Nam, W. Tighe, S. Suckewer, and L. A. Woltz, Proc. SPIE **913**, 164 (1988).
[15] L. A. Woltz and C. F. Hooper, Jr., Phys. Rev. A **38**, 4766 (1988).
[16] W. E. Behring, R. J. Ugiansky, and U. Feldman, Appl. Opt. **12**, 528 (1973).
[17] W. E. Behring, J. H. Underwood, C. M. Brown, U. Feldman, J. F. Seely, F. J. Marshall, and M. C. Richardson,

Appl. Opt. **27**, 2762 (1988).
[18] C. M. Brown, J. O. Ekberg, J. F. Seely, and U. Feldman, J. Opt. Soc. Am. B **6**, 1650 (1989).
[19] S. Goldsmith, J. C. Moreno, H. R. Griem, L. Cohen, and J. Knauer, J. Opt. Soc. Am. B **6**, 1972 (1989).
[20] J. C. Moreno, S. Goldsmith, H. R. Griem, L. Cohen, and J. Knauer, J. Opt. Soc. Am. B **7**, 704 (1990).
[21] B. L. Henke, S. L. Kwok, J. Y. Uejio, H. T. Yamada, and G. C. Young, J. Opt. Soc. Am. B **1**, 818 (1984); B. L. Henke, F. G. Fujiwara, M. A. Tester, C. H. Dittmore, and M. A. Palmer, *ibid.* **1**, 828 (1984).
[22] J. C. Moreno, in *Spectral Line Shapes, Volume 6*, edited by L. Frommhold and J. W. Keto, AIP Conf. Proc. No. 216 (AIP, New York, 1991), p. 127.
[23] H. R. Griem, *Spectral Line Broadening by Plasmas* (Academic, New York, 1974).
[24] A. Calisti, F. Khelfaoui, R. Stamm, B. Talin, and R. W. Lee, Phys. Rev. A **42**, 5433 (1990).
[25] C. A. Iglesias, J. L. Lebowitz, and D. MacGowen, Phys. Rev. A **28**, 1667 (1983).
[26] R. W. Lee, in *Atomic Processes in Plasmas*, edited by E. S. Marmar and J. L. Terry, AIP Conf. Proc. No. 257 (AIP, New York, 1992), p. 39.